PHASE OBJECT OBSERVATION SYSTEM BASED ON DIFFRACTION PHASE MICROSCOPY

Sylwia Babicz, Barbara Stawarz-Graczyk, Paweł Wierzba

Gdańsk University of Technology, Faculty of Electronics, Telecommunications and Informatics, G. Narutowicza 11/12, 80-233 Gdańsk, Poland (✉ sylwia.babicz@pg.edu.pl, +48 58 347 1886, barstawa@pg.edu.pl, pawwierz@pg.edu.pl)

Abstract

In the paper authors present a special measurement system for observing phase objects. The diffraction phas microscopy makes it possible to measure the dimensions of a tested object with a nanometre resolution. To meet this requirement, it is proposed to apply a spatial transform. The proposed setup can be based either on a two lenses system (called $4f$) or a Wollaston prism. Both solutions with all construction aspects are described in the paper. To make a full analysis of the object shape the authors developed an accurate image processing algorithm, also presented in the paper.

Keywords: diffraction phase microscopy (DPM), phase objects.

1. Introduction

Several classes of objects are difficult to examine using conventional light microscopy techniques, since they exhibit complete, or almost complete, transparency. Optical fibres and most biological cells are good examples of such objects. Because the refractive index of such objects differs from that of the surrounding medium, their presence affects the phase of a wave-front propagating through them. Therefore, such objects are often referred to as *phase objects*. Several light microscopy techniques capable of visualizing phase objects have been developed [1–4], such as phase contrast (PC) microscopy [1–3] or micro-interferometry [4]. In many applications they are sufficient, providing all the required information about the examined object.

However, the traditional light microscopy techniques often cannot provide quantitative information, especially about parameters related to the surface and volume of examined object, or require some post-processing. It has stimulated the research into methods capable of providing such information. One of such advanced methods is quantitative phase imaging (QPI), that is used to obtain quantitative information on phase objects. In 2006 Gabriel Popescu *et. al* [5–8] first proposed diffraction phase microscopy (DPM) which is a new solution for quantitative phase imaging of different biological structures. The method is based on a phase contrast (PC) microscopy technique which was discovered in the early thirties of the last century by Dutch physicist Frits Zernike [1, 2]. Gabriel Popescu *et. al* presented the potential of proposed method for quantifying nanoscale motions in live cells on an example of red blood cells (RBCs).

The proposed technique uses the principles of common path interferometry and single-shot phase imaging. Light propagating through a transparent phase object (i.e. an RBC) interferes with a reference beam, forming a fringe field in which the phase is encoded into intensity. Quantitative information about the shape and size of the examined phase object can be obtained by processing the fringe pattern using tools routinely employed in the field of optical interferometry. As a result, quantitative information about the structure and size of phase object is obtained. Following, the information can be analysed in the time domain.

While the quantitative phase imaging is performed using diffraction phase microscopy techniques, it can be also performed using techniques derived from interference microscopy [9]. However, the latter techniques must be modified in order to provide the needed quantitative information, since they were developed to be used by a human observer. Since the CCD/CMOS cameras used in these applications have a much smaller field of view, such modification requires the fringe spacing to be substantially reduced, to provide higher measurement resolution in the field of view of the camera. The setup using a Wollaston prism presented in this paper provides the fringe spacing required by QPI. It is more tolerant to large spatial differences of phase introduced by the specimen (i.e. phase differences of several radians in points located a few micrometres apart), since the fringe spacing is about two times larger than that in similar setups described in the literature.

As it was mentioned before, the proposed system based on DPM is adapted to testing phase objects. For instance, the authors of [9] prepared a phase object specimen (Fig. 1) consisting of narrow strips of thin dielectric films which were evaporated in vacuum on the glass side and then covered with a high-dispersion liquid and a cover slip.
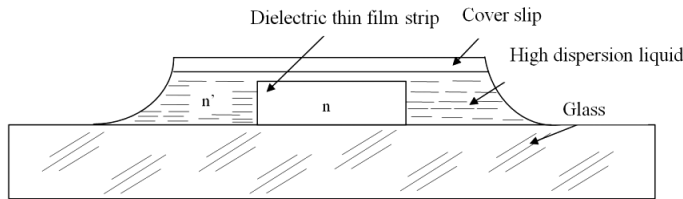

Fig. 1. A specimen for system testing [9].

In general, the immersion specimen should be as thin as possible, which enables to acquire a good quality image and facilitates interpretation of the results and determination of resolution. The choice of immersion liquid assures the refractive index difference between the specimen and the liquid being close or identical to that between the examined object (e.g. cell) and its environment (e.g. solution).

2. Measurement systems

The examination of a phase object can be carried out in several alternative measurement systems which enable the image registration. Measurement systems for examination of a biological cell should provide dimensional resolution in the order of tens of nanometres. The best implemented systems are based on microscopes. The diffraction phase microscope is a good candidate. The microscope can be supplemented with a two-lens image processing system (called $4f$) or a Wollaston prism. In both cases the specimen is illuminated by a laser beam and the recorded image contains a fringe field modified by the examined object. To make a full analysis of the

object shape, it is necessary to create an accurate image processing algorithm. It is proposed by the authors in this paper.

First, a measurement setup with the $4f$ systems presented in [10] was developed. It uses a phase contrast (PC) microscopy technique where the light propagating through a specimen (phase object) interferes with a reference beam, forming a fringe field in which phase is encoded into intensity.

The quantitative information about the shape and size of an examined phase object can be obtained by processing the fringe pattern using tools routinely employed in the field of optical interferometry. Following, this information can be analysed in the time domain. The proposed measurement system uses an interferometer based on diffraction grating and Fourier optics methods to obtain the phase contrast image. It is based on simple and commonly known elements: laser, lenses, diffraction grating and pinhole. The examined object is illuminated by a green solid-state laser ($\lambda = 532$ nm) operating with a lens focusing the light beam. The beam properties were measured with a beam profiler and a Shack-Hartmann sensor. The intensity profile with energy distribution close to that of a Gaussian beam (correlation better than 97%) with a slight ellipticity of the beam were measured, as shown in Fig. 2.
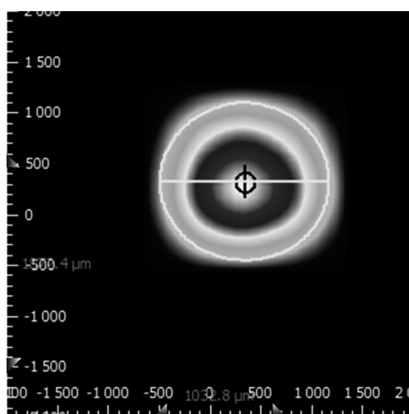

Fig. 2. Measurement of the beam properties.

The wave-front recorded with the Shack–Hartmann sensor does not show sharp discontinuities and is close to that of a Gaussian beam. When discussing the DPM with a Wollaston prism it should be remembered that the two interfering wave-fronts come from regions in the object plane that are separated by 15 to 40 micrometres. In order to affect the DPM operation, the laser beam should have substantial phase fluctuations in these distances. The measurements do not show the presence of such fluctuations.

The image of an examined specimen is created by the microscope objective, having magnification in a range 40x–60x, on the diffraction grating surface. Two beams emerging from the grating – the zeroth-order and the first order beams become reference and imaging beams, respectively. The first lens performs the Fourier transform of both beams. The zeroth-order beam is filtered in the Fourier plane by the pinhole that allows only the plane wave component to pass, while the first-order beam propagates through the round aperture unfiltered. Other beams emerging from the grating are blocked by the screen in which the aperture and the pinhole are placed. The second lens performs the inverse Fourier transform of both beams, which then interfere on the CCD/CMOS camera. This setup is often referred to as a $4f$ optical processor, and can pro-

vide additional magnification (around 4x in most cases) depending on the focal length ratio of the lenses.

Therefore, the light passing through a specimen undergoes only a phase shift, shown schematically in Fig. 3a. When such light is brought to interference with a reference beam having a plane wave-front, an interference fringe field is created (Fig. 3a, right) when the phase relationship between the two beams is stable (i.e. there is adequate spatial and temporal coherence).
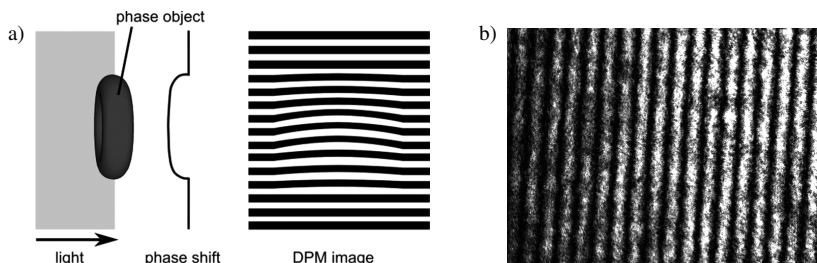

Fig. 3. a) A scheme of creating a DPM image. b) Fringes corresponding to the interference of two plane waves.

The fringe spacing depends on the wavelength of light and on the angle between directions of propagation of the interfering beams. Any change in the fringe pattern from the straight parallel (corresponding to the interference of two plane waves) (Fig. 3b) is caused by the phase shift introduced by the object, and is proportional to its thickness and refractive index. Therefore, it is possible to find the 2D profile of phase change and estimate the phase object thickness from the deflection of the fringes. If the phase object is flickering [11–13] it can be examined by recording a series of images, calculating the phase object size and thickness distributions as functions of time and studying selected characteristics of these distributions.

While this system is an elegant solution, it is quite sensitive to the placement of the optical components. In particular, a suitable placement of the pinhole is critical to its operation. When built from typical laboratory optical and mechanical components and employed in laboratory conditions, the system can easily drift out of alignment due to vibrations and drifts. This can hamper measurements and make any signal processing difficult.

Due to these disadvantages of the DPM measurement setup based on a $4f$ system, the authors decided to develop a DPM measurement setup based on a Wollaston prism. In the new setup the required fringe field is obtained in a much simpler setup consisting of optical elements that are easier to adjust. In the Wollaston prism setup the laser beam goes through the examined object and is reflected by a mirror. Then the beam passes through a shutter, a polarizer, the Wollaston prism and an analyser. As in the previous system, the final image is created on the digital camera. The system based on a Wollaston prism is presented in Fig. 4.

Still, in the design of DPM measurement system based on a Wollaston prism the authors faced some problems. First of them are speckles in the resulting image (Fig. 5). The speckles come either from undesirable laser light reflections inside the objective, or from diffraction on irregularities in the lens surfaces. Some of them are contributed by the laser beam quality. Theoretically, the laser beam should be well-collimated single transverse mode beam. In practice, the lenses used to collimate it introduce some irregularities. Consequently, the interference contrast of the image can vary locally, making the image processing difficult. In spite of using several laser modules operating at 532 nm and several different microscope objectives, the quality of the pictures was not satisfactory. Part of the problem may be caused by the auto-set features of the camera, but the problem with speckles is clearly visible.
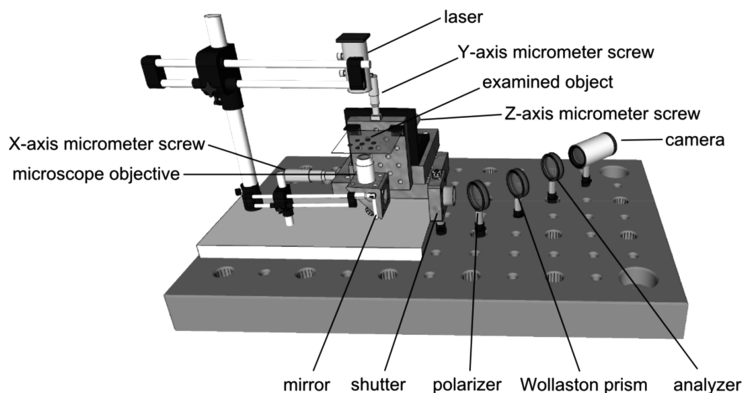
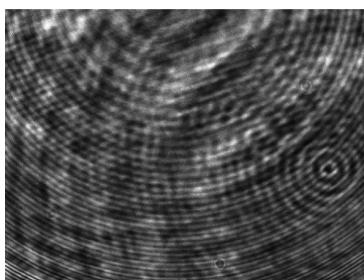Fig. 4. A layout of the DPM measurement setup with a Wollaston prism.

Fig. 5. An example of image created on the camera.

In the reference image (Fig. 6a) another important problem was revealed. The edges of the fringes are blurred. The blur is an effect of interference of two flat wave-fronts with different phase, which results in a sinusoidal-type fringes' pattern. Such a characteristic is not unequivocal for edge detecting algorithms. Thus, a step which must be carried on before any edge analysis, is thresholding, with e.g. the Otsu method [14].
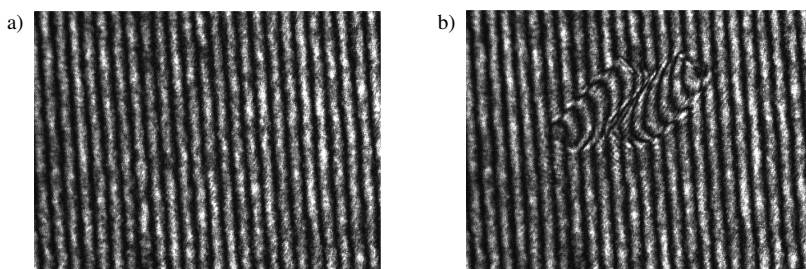

Fig. 6. a) The reference fringe field. b) A tested specimen image.

The authors suppose that it is caused by too narrow a spectrum of the laser beam. Due to the blurred fringes it is almost impossible to properly analyse the small size of the examined object. The best (in the authors' opinion) example of tested specimen images is presented in Fig. 6b.

217

3. DPM phase object simulation software

The phase object simulation and its detection algorithm were evaluated in the Matlab software. The authors did not use any commercial software and toolboxes. All functions were designed and implemented as the authors' original contribution. The aim of the simulation is to detect the phase object edges. Thus, we assume that the distribution of the cells' thickness is a triangle between the edges in the vertical direction. Such a phase object model is presented as a white-black colour image (Fig. 7). The edges of the phase object are treated as ideal vertical brinks. In further works, to detect full phase object fluctuations in three dimensions, the changes of thickness should be also considered. Due to the CCD/CMOS detector resolution, all images have a 1328×1024 px dimension, which corresponds to the detector resolution during recording 120 8-bit mono image frames per second.
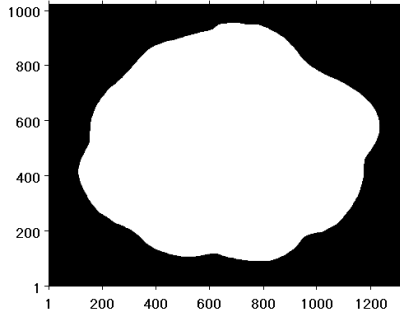

Fig. 7. A prototype image of a phase object.

As in most interferometric techniques using fringe field images, a proper fringe spacing is important. Too wide fringes reduce the accuracy of edge detection, compared with more dense fringes, as illustrated in Fig. 8 using simulated DPM images of phase objects. Moreover, discontinuities in the fringe field can appear when rapid and substantial phase changes exist over small areas of the picture. However, excessive reduction of the fringe spacing can lead to reduction of contrast due to the integrating nature of the pixels of CCD/CMOS detectors. Therefore, the optimum fringe spacing must be a compromise taking into account the aforementioned problems.
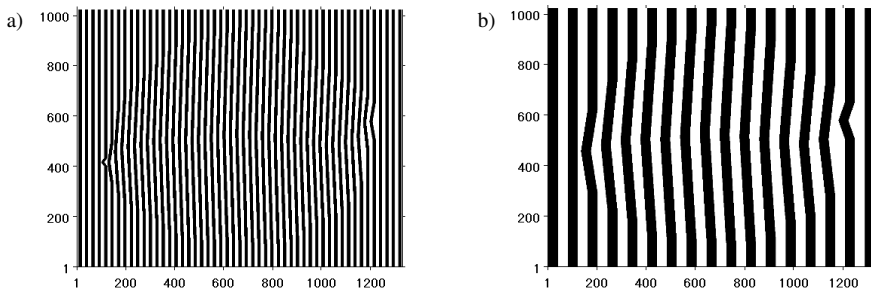

Fig. 8. a) No. 1. b) No. 2. Simulation of phase object images obtained with DPM.

Both Fig. 8a and Fig. 8b images were created for different simulation parameters. The fringes' width of No. 1 image is equal to 1% of the image width rounded to the nearest pixel. The same

width in No. 2 image is equal to 3%. The maximum deflection of fringes is also different and equal to 1% and 2% of the image width (also rounded to the nearest pixel), respectively.

The second part of simulation is to recreate the phase object shape from the DPM images. Because of the different fringes' widths, the number of points representing the edges is greater in picture No. 1 (Fig. 9a). The simulation suggests that the best results will be obtained for narrower fringes. The assertion is correct only for situations, when the biggest fringes' deflection is smaller than the fringes' width. In the opposite situation, the deflected fringes could fuse together what disables detecting the phase object thickness in the future.
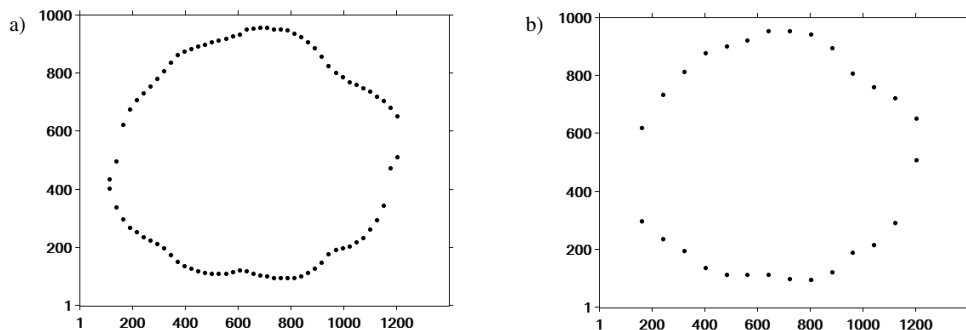
Fig. 9. Recreated points of edges for a DPM image: a) No. 1. b) No. 2.

As the whole system, the software provides measurements of flickering phase objects. The phase object fluctuations in 2D are considered as movement of points in the time domain. The density of points is related to the fringes' width. The best results for fluctuations of edges should be obtained for tiny fringes and an object which does not cause large bending of the fringes. The simulations reveal that, if the full volume fluctuations are considered, the most difficult aspect of the experiment is to select an appropriate fringes' spacing which enables detecting enough points of edges as well as thickness fluctuations of a phase object.

The simulation software was verified in the picture with a testing specimen (Fig. 6b). Firstly, the image was rotated and processed. In Fig. 6b we observe the original testing specimen and its mirror image which overlap each other. To verify the software, only the clear 261×251 px fragment of Fig. 6b was considered (Fig. 10). The positive result of the detection is presented in Fig. 11.
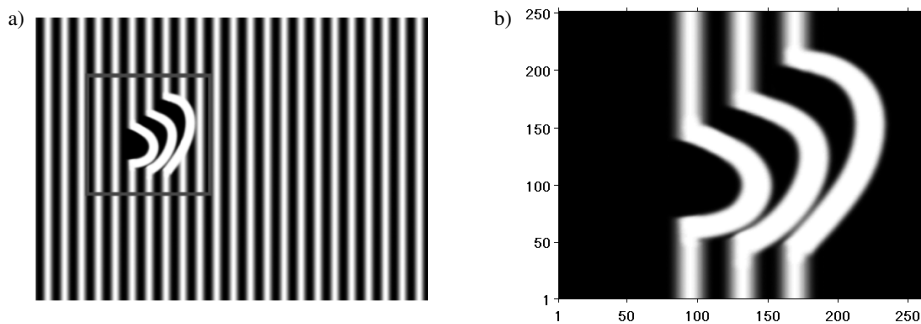
Fig. 10. The rotated (a) and binarized (b) with the marked considered clear fragment of the specimen.
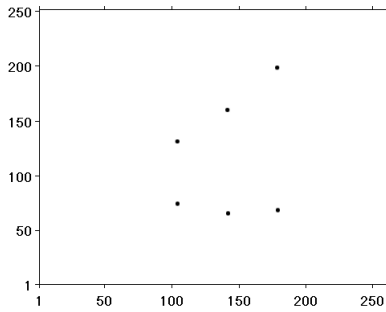
219

Fig. 11. The result of software processing of the considered fragment of Fig. 6b.

4. Conclusions

An experimental system using a microscope objective supplemented by a diffractiongrating-based micro-interferometer was built and tested. Its magnification, being about 160 times, is sufficient for examination of phase object images. The micro-interferometer, using Fourier optics filtering methods, is difficult to align and requires tight mounting tolerances, reducing its usability in the planned research.

Therefore, a second system, using a Wollaston prism to create the fringe field, was designed, built and tested. The system performance was hampered by speckles arising from parasitic reflections and diffraction. Using a source with a wider spectrum reduced these problems and enabled to acquire the fringe field pictures with an acceptable quality. The setup still requires some optimization in order to further improve the image quality. For example, the authors predict that the speckles could substantially be reduced by using a light source with a wider spectrum, such as a laser diode operating in a few longitudinal modes.

The further research will be aimed at developing and optimizing effective methods for converting the interferogram into information about the phase object. Another important part of the future work is to simulate 3D phase object images obtained with DPM and recreate the full shape of the specimen. The simulation can prove that it is possible to analyse each frame of the movie as a single step during considering the phase object fluctuations. Such phenomena can evaluate the state of red blood cells and are very sensitive to the presence of any compounds in blood. Changing the position and bending the fringes in a DPM image provides sufficient information for studying of flickering only if the fringes' spacing is properly selected.

We suppose that this method can be even more sensitive than the Raman spectroscopy for detection of chemical compounds or their remnants (e.g. [15]) in red blood cells by inducing characteristic low frequency fluctuations and should be much cheaper than this competitive method [16]. Numerous papers confirmed that noise (especially flicker noise) is very sensitive to any environmental changes in various phenomena and can induce non-Gaussian noise [17, 18].

References

[1] Zernike, F. (1942). Phase contrast, a new method for the microscopic observation of transparent objects. *Physica*, 9(7), 686–698.

[2] Zernike, F. (1942). Phase contrast, a new method for the microscopic observation of transparent objects part II. *Physica*, 9(10), 974–980.

[3] Burch, C.R., Stock, J.P.P. (1942). Phase-Contrast Microscopy. *J. of Sci. Instr.*, 19(5), 71–75.

[4] Hariharan, P. (2010). *Basics of interferometry*. Academic Press.

[5] Popescu, G., Ikeda, T., Dasari, R.R., Feld, M.S. (2006). Diffraction phase microscopy for quantifying cell structure and dynamics. *Opt. Lett.*, 31(6), 775–777.

[6] Park, Y., Popescu, G., Badizadegan, K., Dasari, R.R., Feld, M.S. (2006). Diffraction phase and fluorescence microscopy. *Opt. Exp.*, 14(18), 8263–8268.

[7] Bhaduri, B., Edwards, C., Pham, H., Zhou, R., Nguyen, T.H., Goddard, L.L., Popescu, G. (2014). Diffraction phase microscopy: principles and applications in materials and life sciences. *Adv. in Opt. and Phot.*, 6(1), 57–119.

[8] Bhaduri, B., Pham, H., Mir, M., Popescu, G. (2017). Diffraction phase microscopy with white light. *Opt. Lett.*, 37(6), 1094–1096.

[9] Pluta, M. (1989). *Advanced light microscopy. Vol. 2: Specialized Methods*. PWN, Elsevier.

[10] Babicz-Kiewlicz, S., Stawarz-Graczyk, B., Wierzba, P., Mazikowski, A. (2015). Diffraction Phase Microscopy for observation on red blood cells fluctuation. *Zeszyty Naukowe Wydziału Elektrotechniki i Automatyki Politechniki Gdańskiej*, 46, 13–16.

[11] Majeed, H., Sridharan, Sh., Mir, M., Ma, L., Min, E., Jung, W., Popescu, G. (2017). Quantitative phase imaging for medical diagnosis. *J. of Biophot.*, 10(2), 177–205.

[12] Popescu, G., Park, Y., Choi, W., Dasari, R.R., Feld, M.S., Badizadegan, K. (2008). Imaging red blood cell dynamics by quantitative phase microscopy. *Blood Cells, Molecules, and Diseases*, 41(1), 10–16.

[13] Pham, H.V., Bhaduri, B., Tangella, K., Best-Popescu, C., Popescu, G. (2013). Real Time Blood Testing Using Quantitative Phase Imaging. *PloS one*, 8(2), e55676.

[14] Otsu, N. (1979). A threeshold selection method from gray-level histograms. *IEEE Trans. on Systems, Man and Cybernetics*, 9(1), 62–66.

[15] Kwiatkowski, A., Czerwicka, M., Smulko, J., Stepnowski, P. (2014). Detection of denatonium benzoate (Bitrex) remnants in noncommercial alcoholic beverages by Raman spectroscopy. *Journal of Forensic Sciences*, 59(5), 1358–1363.

[16] Gnyba, M., Smulko, J., Kwiatkowski, A., Wierzba, P. (2011). Portable Raman spectrometer-design rules and applications. *Bulletin of the Polish Academy of Sciences: Technical Sciences*, 59(3), 325–329.

[17] Smulko, J., Darowicki, K. (2003). Nonlinearity of electrochemical noise caused by pitting corrosion. *Journal of Electroanalytical Chemistry*, 545, 59–63.

[18] Lentka, Ł., Smulko, J.M., Ionescu, R., Granqvist, C.G., Kish, L.B. (2015). Determination of gas mixture components using fluctuation enhanced sensing and the LS-SVM regression algorithm. *Metrol. Meas. Syst.*, 22(3), 341–350.